FROM THE LABORATORY OF RADIATION PHYSICS (DIRECTOR: C. B. MADSEN), RADIUM CENTRE, DK-8000 ÅRHUS, DENMARK.

MEASUREMENTS OF SINGLE EVENT SPECTRA WITH A WALL-LESS PROPORTIONAL COUNTER IN LOW LET RADIATION FIELDS

K. A. JESSEN

It is generally accepted that knowledge of the distributions of energy absorbed by microscopic sites is necessary for the understanding of the response of a cell exposed to radiation. The technique for measuring such distributions has been introduced several years ago (ROSSI & ROSENZWEIG 1955). The measurements are normally performed by simulating microscopic volumes with tissue equivalent gases at low pressure in proportional counters with walls of tissue equivalent materials.

Measurements in low LET radiation fields of high energy roentgen and gamma rays have been scarce, especially in fields for radiation therapy (LINDBORG 1974). Two of the main problems in measuring distributions in radiation fields are the high photon fluences and the wall effects in the detector.

Measurements of single event distributions have been performed with a wall-less dipole proportional counter in ^{60}Co gamma ray fields from a point source and in collimated roentgen ray fields from a 6 MV Varian linear accelerator, and the results are now reported.

The probability distributions in event sizes P(Y) are measured in these fields at gas pressures which simulate spheres with diameters of 0.5 μm, 1 μm, and 2 μm tissue. The event size Y is defined as the quotient of energy deposited by an event ε in a

Submitted for publication 2 July 1975.

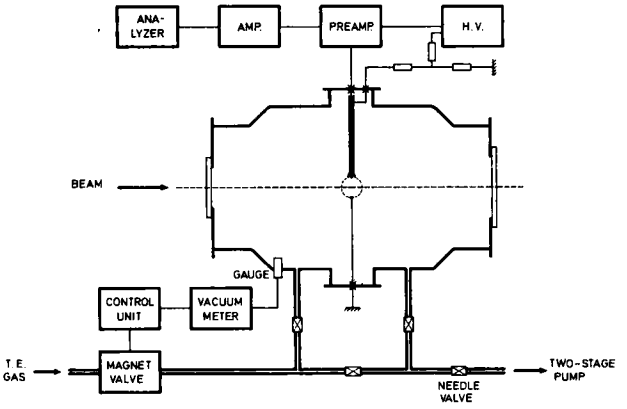

Fig. 1. The experimental arrangement (not in scale).

spherical volume of diameter d by d, $Y = \varepsilon/d$. Also energy deposition spectra are presented for the two radiation qualities. The deviations in these spectra are not sufficient for conclusions about significant differences in microscopic energy deposition for the two qualities, taking the differences in the measuring geometries into account.

Calculations of the relative variance in LET are performed for the radiation sources used and for different cut-off energies corresponding to different diameters or cord lengths in the detector. These values are compared with the relative variance of the measured distributions which shows that only for small sites the LET part in the variance could be greater than the contribution from the straggling.

Description of the apparatus

The detector. The experimental arrangement is illustrated schematically in Fig. 1. The wall-less proportional counter used is a so-called martini counter (GLASS & BRABY 1969), whose boundaries are determined by a spherically shaped electric field. This field is performed by two exactly spherical electrodes of stainless steel, 0.8 mm in diameter (SKF balls). The electrodes are supported by two cannula pipes of stainless steel and with an outer diameter of 0.42 mm. The counter cathode is connected to ground potential and the anode is connected to a high voltage supply, working in the potential range 700 V to 1 100 V, depending on the gas pressure used. The potential should be sufficiently high to get reasonable gas multiplication ($\approx 10^4$) and homogeneous collection of the free electrons formed in the spherical volume without recombination, and well below the limit for breakdown of the counting gas. The separation between the two electrodes is 20 mm.

For defining the spherical shape the collecting volume for electrons is limited by a guard electrode. This electrode consists of a glass pipe containing the anode support and ending in a hemispherical cup with a diameter of 2.5 mm and with the anode placed at the center. The glass pipe is coated and made conductive with a thin layer

of silver on the outside. The potential of the guard electrode is adjusted so that the silver layer on the hemispherical cup fits an equipotential surface of the dipole field. The potential of the guard electrode is about 20 per cent of the anode potential. The two critical parameters, the position of the anode in the guard cup and the potential of the guard electrode, were optimized by using a collimated beam of 5.3 MV α-particles from an open ^{210}Po source. The collimated α-beam was crossing the detector along different diameters for checking the spherical collecting volume. Due to the rotational symmetry about the axis defined by the supports of the electrodes, investigations are only performed in one of the plans containing this axis. The α-source was placed on a median up to $\pm 60^0$ from the central diameter between the electrodes and deviations in the measured pulse high were less than ± 6 per cent. The electrode supports are fixed to perspex sockets for alignments.

The vacuum chamber system. The vacuum chamber is a 75×10^{-3} m^3 cylindrical container of stainless steel and with a diameter of 0.4 m. On the end-flanges are mounted perspex windows (thickness: 5–20 mm) for exposure to external sources. As counting gas is used a tissue equivalent gas mixture composed by volume of 64.4 per cent CH_4, 32.4 per cent CO_2, and 3.2 per cent N_2. The counter is operated with a gas flow down to 30 mm$^3 \times$ s^{-1} (atmospheric). The design of the gas flow system is schematically represented in Fig. 1. To maintain a constant and low pressure in the chamber, an electromagnetic valve (Balzer RME010 and valve control unit RVG040) is inserted between the gas container and the chamber. The valve is controlled by a pirani gauge (Balzer TPR010) which measures the pressure in the chamber. For controlling the absolute pressure and the gas dependency of the pirani at higher pressure, a mercury manometer is used (Struers USA-manometer). For reducing the gas flow rate a needle valve is employed between the chamber and the foreline traps for the rotary pump (Balzer DUO008). During all measurements the pressure was constant within 0.2 per cent. The rotary pump was mechanically separated from the chamber system for neutralizing vibrations at the electrodes which considerably reduced the electronic noise level.

Electronics. The counter was connected directly to a charge-sensitive preamplifier (ORTEC 109PC) with a short cabel. The capacity of the cabel and the detector is 25 pF which gives a noise level of about 450 e^-_{rms}. The limiting effect of the electronic noise is defined by the root mean square (rms) of electrons which represent the preamplifier noise. The signals are then fed to a linear amplifier (ORTEC 452) with pulse shaping facilities. Normally a bipolar pulse shaping and a shaping time constant of 3 μs are used. Finally, the pulses were fed to the ADC of a multichannel analyzer (Northern Scientific, 4096 channels). The linearity of the electronic system was checked with a precision pulser.

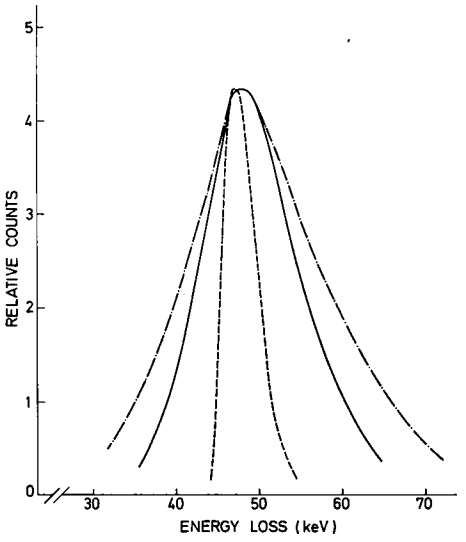

Fig. 2

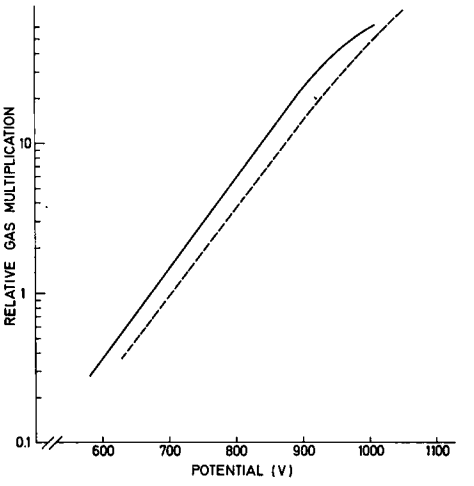

Fig. 3

Fig. 2. Measured distributions of 5 MeV collimated α-particles in 0.5 μm simulated tissue layer for different collimator sizes. The beam covers 12.5 per cent (—) and 40 per cent (—·—) of the solid angle for the detector volume. The dotted line (– – –) is the Vavilov distribution for a perfectly collimated beam of α-particles at the same energy.

Fig. 3. The relative gas multiplication as a function of anode voltage for two different gas pressures: 2.67×10^3 N·m^{-2} (—), and 6.67×10^3 N·m^{-2} (– – –).

Calibration and test measurements

For testing, the detector was exposed to 5.3 MeV α-particles from a thin layer of ^{210}Po on a Ni-foil, which gives nearly monoenergetic α-particles. The foil was placed in a collimating device 115 mm from the center of the detector and assumed not to disturb the fields in the detector.

Two distributions measured after optimizing the spherical field shape appear in Fig. 2. The beam of α-particles is covering 12.5 percent and 40 per cent, respectively, of the area of the circle defined by the electrodes and in a plan perpendicularly to the beam. As a theoretical limit the Vavilov distribution (SELTZER & BERGER 1964) is also presented in Fig. 2 for 5.0 MeV α-particles traversing a thin T.E. gas layer, simulating 0.5 μm tissue with a calculated energy loss of 48.6 keV (BARKAS & BERGER 1964).

Fig. 3 gives the relative gas multiplication as a function of the anode voltage for two typical gas pressures used in the measurements, 2.67×10^3 N·m^{-2} (20 torr), and 6.67×10^3 N·m^{-2} (50 torr). The pulse height distribution is measured for the α-particles at different voltage. The figure illustrates the exponential multiplication in the applied voltage range and the beginning of gas breakdown is suggested only for the low pressure curve.

The energy calibration is performed by using the beam of α-particles for the three gas pressures applied, simulating volumes with diameters of 0.5 μm, 1 μm, and 2 μm tissue. The energies of the α-particles at the center of the detector and the energy losses in the three simulated volumes were calculated following tables given by BARKAS & BERGER.

The calibration was tested for lower energies using a ^{55}Fe source placed near to the detector and producing photoelectrons at 5.88 keV in the counting gas. This test could only be performed with a gas pressure higher than used in the measurements ($\geqslant 10^4$ N·m^{-2}) because the range of the photoelectrons should be less than the simulated volume to get a reasonable peak. This test was performed with a gas pressure at 10^4 N·m^{-2} simulating about 2 μm tissue and yielded an energy deposition of 122.5 eV per channel compared with 122.7 eV per channel for the α-particles, which means an agreement within the experimental uncertainty.

The resolution of the detector for ^{55}Fe measured at the high pressure ($\sim 2.5 \times 10^4$ N·m^{-2}) is about 24 per cent, but the relatively poor resolution of this counter should not be the critical factor in measuring event spectra (KELLERER 1968 a).

Measurements of single event spectra

For measurements of the event spectra for ^{60}Co gamma radiation a point source of 20 MBq ($\sim$0.5 mCi) is placed near to the perspex window (5 mm thick) outside the chamber and in a distance of 0.3 m from the detector. Measurements on a ^{60}Co therapy unit was attempted but it was not possible to reduce the photon fluence sufficiently to avoid pile-up pulses. The background level in the therapy room was also a serious problem when the source was open.

For measurements on the linear accelerator, pile-up plays an important role, but here it is possible to place the measuring chamber 10 m from the target and with a 1.6 m thick wall of heavy concrete between the target and the detector to reduce the background level below 5 counts per second. The pulsed radiation has a frequency of 200 Hz for the dose rate used in these measurements and a pulse length of about 3 μs. It is possible to introduce cylindric collimators of lead in both ends of the beam port through the wall for reducing the photon fluence. The diameter of the second collimator after the target is constructed in such a way that no interaction with the primary beam passing the first collimator occurs. The distance of 4 m between the second collimator and the chamber should prevent collimator effects in the detector. Diameters from 6.4 to 1.2 mm was used for the first collimator which gives solid angles from 2×10^{-6} sr to 6×10^{-8} sr for the radiation beam from the target and typical count rates in the detector from 1 000 s^{-1} to 30 s^{-1}. This means that only for the smallest collimator the pile-up is negligible. The chamber is aligned to let the beam pencil cross the detector between the electrodes.

It is assumed in the measurements of single event spectra that the size of a pulse from the counter is directly proportional to the number of primary ions formed in an event and thus to the energy deposition in the simulated spherical volume by this

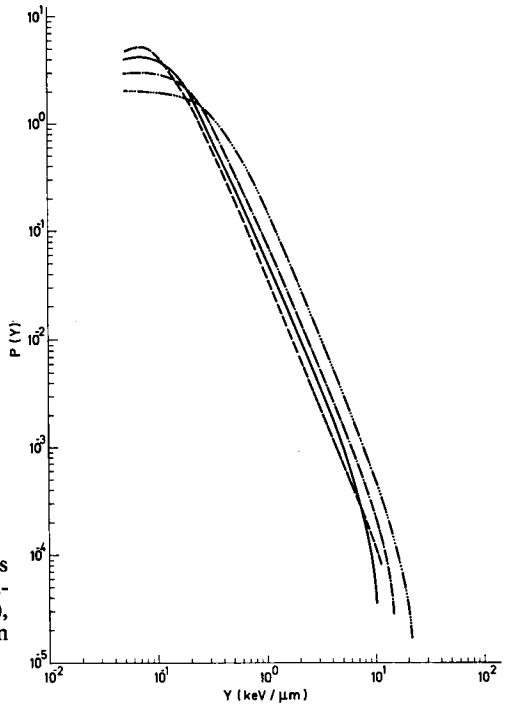

Fig. 4. The energy deposition probability curves for ^{60}Co gamma radiation in spheres with simulated diameters of 2.0 μm (—), 1.0 μm (—·—), and 0.5 μm (–· · ·–) tissue and for 6 MV roentgen radiation in 1.0 μm (– – –).

event. Fig. 4 presents the energy deposition probability curves measured for broad gamma beams from the ^{60}Co point source for pressures corresponding to spheres of tissue of 2.0 μm, 1.0 μm, and 0.5 μm in diameter, and for collimated 6 MV roentgen rays at 1.0 μm. The results are presented in terms of event size Y, and P(Y) is the normalized probability distribution (KELLERER & ROSSI 1970).

The probability is increasing for larger event sizes as the diameter of the sphere is decreasing. This means that the interactions tend to be more definitely alternative for smaller sites, i.e. more electrons are passing the sphere without any interaction. The curve for the 6 MV roentgen rays (Fig. 4) reveals that the probability is decreasing for increasing energy of the incoming gamma photons which produce more energetic electrons with lower LET values.

Fig. 5 illustrates the energy deposition spectra for the two radiation sources in a simulated sphere of 1 μm. $D(Y) = P(Y) \cdot Y$ is the normalized absorbed dose distribution in event sizes. It illustrates the shift in energy deposition for the two sources through lower energy depositions for the 6 MV roentgen rays due to the more energetic electrons. The difference in beam geometry would probably also contribute to the deposition shift, especially the influx into the counter volume of δ-electrons with higher deposition events would be of more importance in the broad beam geometry.

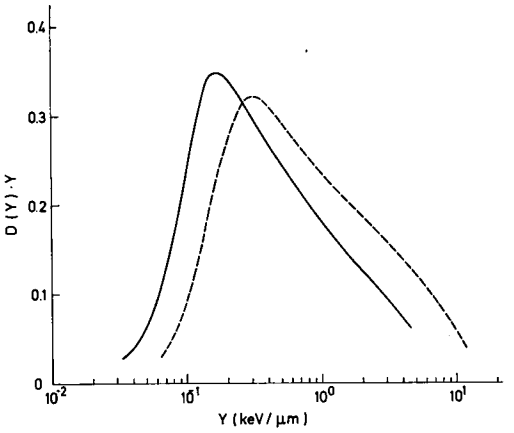

Fig. 5. The energy deposition spectra in 1 μm simulated tissue for 6 MV roentgen radiation (—) and ^{60}Co gamma rays (– – –).

In Table 1 the absorbed dose and the number averages of event sizes $\bar{Y}_D$, and $\bar{Y}_P$ for the measured event spectra are listed.

The agreement between these ^{60}Co data is good, especially for the 2 μm sphere. The differences for smaller sites are probably due to greater uncertainties in the data for these sites and not to the wall effect because this effect will contribute to larger event (GLASS & GROSS 1972). The shift for the two radiation qualities is clearly indicated in the data.

Comparison with LET values and discussion

It can be shown that for the relative variance V in a measured single event distribution the following relation holds (KELLERER 1968) whenever the particle tracks are long compared to the volume of interest:

$V = V_{track} + V_{LET} + V_{track} \cdot V_{LET} + V_{straggling} + V_{gas\ counter} \cdot V_{track}$ is the relative variance of the chord length distribution and the value 0.125 is normally used for a spherical volume. The other terms are obvious. Another relation for the relative variance

Table 1

The number and the dose averages of event sizes $\bar{Y}_P$ and $\bar{Y}_D$ measured for three simulated spheres of tissue in the two radiation fields. The figures in parenthesis are data reported by BIAVATI & BOER. *V is the relative variance of the single event distributions*

Size (μm)	$\bar{Y}_P$ keV/μm		$\bar{Y}_D$ keV/μm		$V = \frac{\bar{Y}_D}{\bar{Y}_P} - 1$	
	^{60}Co	6 MV	^{60}Co	6 MV	^{60}Co	6 MV
0.5	0.54 (0.496)	0.21	2.32	1.21	3.3	4.6
1.0	0.32 (0.262)	0.18	1.38 (1.240)	0.86	3.3	3.8
2.0	0.24 (0.230)	0.13	1.00 (0.982)	0.64	3.2	4.1

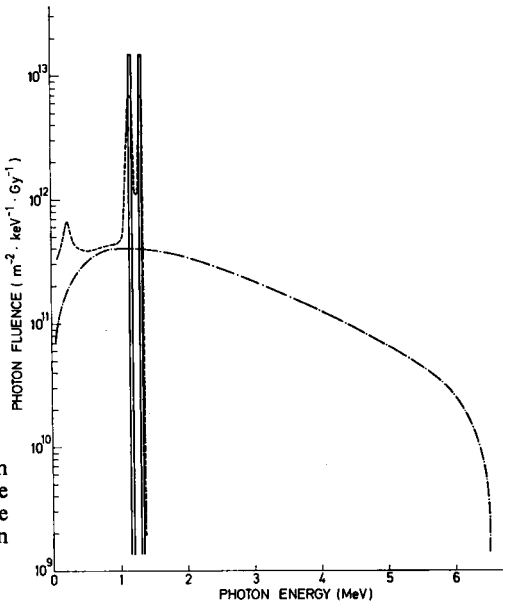

Fig. 6. Three photon spectra normalized to an absorbed dose of 1 Gy (=100 rad) in tissue equivalent gas. ^{60}Co γ radiation: point source (—), therapy unit (– – –), 6MV roentgen radiation (—·—).

given by directly measured quantities is $V = \bar{Y}_D/\bar{Y}_P - 1$, and a corresponding relation may be given for the relative variance of the LET distribution $V_{LET} = \bar{L}_{\Delta,D}/\bar{L}_{\Delta,T} - 1$, where $\bar{L}_{\Delta,D}$ is the absorbed dose average in LET and $\bar{L}_{\Delta,T}$ is the track average in LET. Δ is the cut-off energy.

The relative variance of LET is calculated for three cut-off energies and for three different spectral distributions (Fig. 6), measured previously (JESSEN 1973). These distributions are normalized to an absorbed dose of 1 gray (1 Gy = 100 rad, CGPM 1975) and used for calculations of the initial electrons set in motion in the tissue equivalent gas.

From the primary electron spectra the slowing down spectra are calculated by means of MCGINNIES' tables (NBS 597, 1959). The table for water is applied in the calculations due to the small differences of the two parameters Z/A and I, the mean

Table 2

The relative variance in LET $V_{LET} = \bar{L}_{\Delta,D}/\bar{L}_{\Delta,T}$ calculated for three cut-off energies and radiation sources

Δ (keV)	^{60}Co Point source	^{60}Co Therapy unit	6 MV Roentgen-rays
2.5	2.39	2.36	2 55
3.6	1.73	1.72	1.80
5.1	1.21	1.21	1.23

excitation-ionization potential, for water and tissue equivalent gas. $Z/A = 0.555$ and 0.542, and $I = 65.1$ eV, and 62.9 eV, respectively. The calculation procedure follows the method described previously (ENNOW & JESSEN 1975), but the higher cut-off energies overcome the problems with the binding energies of the K-electrons.

From the slowing down spectra the relative variance in LET could be calculated and the V_{LET} values for the different radiation sources and cut-off energies are listed in Table 2. For a certain energy cut-off there seems to be no significant deviations in V_{LET} for the three sources. The cut-off energies are related to the electron ranges in tissue equivalent gas in such a way that a 5 keV electron has a range equal to the diameter of the detecting sphere at 1 μm.

The values of the relative variance of the measured event distributions (also listed in Table 1) could be compared with the relative variance of the LET values. V_{LET} increases for decreasing simulated volumes. The total relative variance seems to be rather independent of volume but has increasing tendency for higher photon energies probably due to the straggling term.

Assuming that the relative variance of the counter (KELLERER 1968) is of the order comparable to V_{track} then $V_{straggling}$ must be the dominant term in the rest of the variance and for volumes above 1 μm also more important than V_{LET}. Further measurements with other geometries and detector constructions are needed to determine significant differences in the energy deposition for the two radiation qualities.

Acknowledgements

The author wishes to thank Dr. C. B. Madsen for available encouragement and support in this work and Prof. T. Andersen for many helpful discussions about details. He also wishes to extend his appreciation to the staff of the institute of physics and the laboratory of radiation physics for co-operation particularly to S. E. Pedersen for his excellent performance of the measuring chamber. The work received the financial support of the Danish Medical Research Council. The calculations were performed on the CDC-6400 computer at the University of Aarhus.

SUMMARY

Measurements have been made on ^{60}Co gamma rays from a point source and on 6 MV roentgen rays from a linear accelerator with a wall-less proportional counter. Single event spectra have been measured in sites of 0.5–2 μm in diameters simulated with a tissue equivalent gas. Calculations of the relative variance in LET are performed and compared with the relative variance of the measured distributions for estimates about the straggling contribution.

ZUSAMMENFASSUNG

Es wurden Messungen an ^{60}Co Gamma Strahlen von einer Punktquelle und an 6 MV Röntgenstrahlen von einem Linearaccelerator mit einem Wand-losen Proportionel-Rechner vorgenommen. Es wurden Spektren von einzelenen Geschehnissen in Grössen von 0,5–2 μm

im Diameter, die mit einem Gewebe-äquivalenten Gas simuliert worden waren, gemessen. Es wurden Berechnungen der relativen Varians in der LET vorgenommen und mit der relativen Varians der gemessenen Verteilungen für Abschätzungen des Streuung-Beitrags verglichen.

RÉSUMÉ

Des mesures ont été faites avec un compteur proportionnel sans parois sur le rayonnement gamma ^{60}Co émis par une source ponctuelle et sur les rayons de Röntgen de 6 MV émis par un accélérateur linéaire. Les spectres d'événements individuels ont été mesurés dans des régions de 0,5–2 μm de diamètre simulées avec un gaz équivalent aux tissus. Les calculs de variance relative du TLE ont été faits et comparés avec la variance relative des distributions mesurées pour des évalution de la contribution du » straggling ».

REFERENCES

BARKAS W. H. and BERGER M. J.: Tables of energy losses and ranges of heavy charged particles. Nat. Acad. Sci.-Nat. Res. Council, Washington 1964, Publ. No. 1133, p. 103.

BIAVATI M. H. and BOER E.: D(Y) Spectra-gamma rays. Report. NYO-2740-3, Radiological Research Laboratory, Columbia University, New York 1966.

CGPM: The 15th General Conference on Weights and Measures, May 1975.

ENNOW K. and JESSEN K. A.: Spectral measurements and Monte Carlo calculations of scattered radiation from therapeutic radiation sources. Acta radiol. Ther. Phys. Biol. 14 (1975), 262.

GLASS W. A. and BRABY L. A.: A wall-less detector for measuring energy deposition spectra. Radiat. Res. 39 (1969), 230.

— and GROSS W. A.: Wall-less detectors in microdosimetry. *In*: Topics in radiation dosimetry. Suppl. 1, p. 221. Edited by F. H. Attix. Academic Press, New York 1972.

JESSEN K. A.: Measurements of primary spectra from a kilocurie Cobalt-60 unit and a 6 MeV linear accelerator. Acta radiol. Ther. Phys. Biol. 12 (1973), 561.

KELLERER A. M. (a): Microdosimetry and the theory of straggling. *In*: Biophysical aspects of radiation quality, p. 89. IAEA, Vienna 1968.

— (b): Local energy spectra and counter resolution. Report NYO-2740-5, Radiological Research Laboratory, Columbia University, New York 1968.

— and ROSSI H. H.: Summary of quantities and functions employed in microdosimetry. *In*: Proc. Second Symp. Microdosimetry. EUR-4452, p. 841. Commission of the European Communities, Brussels 1970.

LINDBORG L.: Microdosimetry in high energy electron and ^{60}Co gamma ray beams for radiation therapy. *In*: Proc. Fourth Symp. Microdosimetry, EUR-5122, p. 799. Commission of the European Communities, Luxembourg 1974.

MCGINNIES R. T.: Energy spectrum resulting from electron slowing down. Nat. Bur. Std. (U.S.) Circ. 597 (1959).

ROSSI H. H. and ROSENZWEIG W.: A device for measurement of dose as a function of specific ionization. Radiology 64 (1955), 204.

SELTZER S. M. and BERGER M. J.: Energy loss straggling of protons and mesons: Tabulation of the Vavilov distribution. Nat. Acad. Sci.—Nat. Res. Council, Washington 1964, Publ. No. 1133, p. 187.